Published OnlineFirst May 3, 2018; DOI: 10.1158/0008-5472.CAN-17-3797

Tumor Biology and Immunology

Cancer Research

The Autotaxin—Lysophosphatidic Acid Axis Promotes Lung Carcinogenesis

Christiana Magkrioti[1], Nikos Oikonomou[1], Eleanna Kaffe[1], Marios-Angelos Mouratis[1], Nikos Xylourgidis[1], Iliana Barbayianni[1], Petros Megadoukas[1], Vaggelis Harokopos[1], Christos Valavanis[2], Jerold Chun[3], Alexandra Kosma[4], Georgios T. Stathopoulos[5,6], Evangelos Bouros[7], Demosthenes Bouros[7], Konstantinos Syrigos[8], and Vassilis Aidinis[1]

Abstract

Pathogenesis and progression of lung cancer are governed by complex interactions between the environment and host genetic susceptibility, which is further modulated by genetic and epigenetic changes. Autotaxin (ATX, ENPP2) is a secreted glycoprotein that catalyzes the extracellular production of lysophosphatidic acid (LPA), a growth-factor–like phospholipid that is further regulated by phospholipid phosphatases (PLPP). LPA's pleiotropic effects in almost all cell types are mediated through at least six G-protein coupled LPA receptors (LPAR) that exhibit overlapping specificities, widespread distribution, and differential expression profiles. Here we use both preclinical models of lung cancer and clinical samples (from patients and healthy controls) to investigate the expression levels, activity, and biological role of the above components of the ATX/LPA axis in lung cancer. *ENPP2* was genetically altered in 8% of patients with lung cancer, whereas increased ATX staining and activity were detected in patient biopsies and sera, respectively. Moreover, *PLPP3* expression was consistently downregulated in patients with lung cancer. Comparable observations were made in the two most widely used animal models of lung cancer, the carcinogen urethane–induced and the genetically engineered *K-ras*^{G12D}–driven models, where genetic deletion of *Enpp2* or *Lpar1* resulted in disease attenuation, thus confirming a procarcinogenic role of LPA signaling in the lung. Expression profiling data analysis suggested that metabolic rewiring may be implicated in the procarcinogenic effects of the ATX/LPA axis in *K-ras*-^{G12D}–driven lung cancer pathogenesis.

Significance: These findings establish the role of ATX/LPA in lung carcinogenesis, thus expanding the mechanistic links between pulmonary fibrosis and cancer. *Cancer Res; 78(13); 3634–44.* ©*2018 AACR.*

Introduction

Lung cancer is the most prevalent form of malignancy and the leading cause of global cancer-related mortality; the prognosis for patients with lung cancer remains dismal, with a 5-year survival rate below 20%, for all disease stages combined. The major (85%) histological subtype of lung cancer is non–small cell lung cancer (NSCLC), which is further subdivided to adenocarcinoma (ADC; 40%), squamous cell carcinoma (SCC; 25%–30%), and large cell carcinoma (LCC; 10%–15%; ref. 1).

The molecular origins of lung cancer lie in complex interactions between the environment and host genetic susceptibility, further modulated by genetic and epigenetic changes, leading to changes in the activation status of oncogenes and tumor suppressor genes (1). However, lung cancer, and especially NSCLC, is considered as a group of distinct diseases with vast genetic and cellular heterogeneity and although some genomic alterations are shared among various histologic types, most alterations remain distinct (2). The identified genomic alterations are not always associated with the activation of the relevant cellular pathways and the corresponding phenotypic aberrations (3), thus further increasing the complexity of correlating genotypic and phenotypic data.

Ectonucleotide pyrophosphatase/phosphodiesterase 2 (ENPP2), more commonly known as autotaxin (ATX), is a secreted glycoprotein widely present in biological fluids. ATX catalyzes the extracellular hydrolysis of circulating and/or *de novo* produced lysophosphatidylcholine (LPC) to lysophosphatidic acid (LPA; ref. 4). LPA, whose levels are catabolized by phospholipid phosphatases (PLPP; ref. 5), is a pleiotropic phospholipid mediator that evokes growth factor–like responses such as cell growth, survival, differentiation and motility, in most cell types (6). The large variety of LPA effector functions is attributed to at least six G-protein coupled LPA receptors (LPAR), exhibiting overlapping specificities and widespread distribution (7). The orphan GPR87 and P2Y10 receptors, as well as the receptor for advanced glycation end products (RAGE) and the intracellular peroxisome proliferator-activated receptor γ (PPARγ), have also been suggested to mediate LPA signaling (4, 7).

[1]Division of Immunology, Biomedical Sciences Research Center "Alexander Fleming," Greece. [2]Department of Pathology, Metaxa Cancer Hospital, Greece. [3]Sanford Burnham Prebys Medical Discovery Institute, La Jolla, California. [4]First Pulmonary Clinic, Papanikolaou General Hospital, Greece. [5]Department of Physiology, Laboratory for Molecular Respiratory Carcinogenesis, Faculty of Medicine, University of Patras, Patras, Greece. [6]Comprehensive Pneumology Center and Institute for Lung Biology and Disease, University Hospital, Ludwig-Maximilian University and Helmholtz Zentrum München, Germany. [7]Academic Department of Pneumonology, University of Athens, Athens, Greece. [8]Oncology Unit, Sotiria Hospital, School of Medicine, University of Athens, Athens, Greece.

Note: Supplementary data for this article are available at Cancer Research Online (http://cancerres.aacrjournals.org/).

Corresponding Author: Vassilis Aidinis, Division of Immunology, Biomedical Sciences Research Center "Alexander Fleming," Fleming 34, 16672 Athens, Greece. Phone: 302109654382; Fax: 302109654210; E-mail: V.Aidinis@Fleming.gr

doi: 10.1158/0008-5472.CAN-17-3797

Published OnlineFirst May 3, 2018; DOI: 10.1158/0008-5472.CAN-17-3797

ATX was originally isolated as an autocrine motility stimulation factor from the supernatant of metastatic melanoma cells; because increased ATX expression has been detected in several chronic inflammatory and/or malignant diseases (4, 8). ATX expression and LPA production have been shown to be essential for embryonic development (9), but largely dispensable for adult life (10), suggesting ATX/LPA as a developmental pathway aberrantly reactivated in pathophysiological situations. Transgenic overexpression of ATX or LPARs specifically in the mammary gland resulted in spontaneous breast cancer in aged mice (11), suggesting that ATX/LPA may amplify oncogenic age-related signals. Moreover, conditional genetic deletion of ATX from hepatocytes was recently shown to attenuate the development of both liver fibrosis and hepatocellular carcinoma (HCC; ref. 12).

Increased ATX and LPA levels have been identified in the lung tissue and bronchoalveolar lavage fluid (BALF), respectively, of patients with idiopathic pulmonary fibrosis (IPF), whereas genetic deletion of *Enpp2* or *Lpar1* have been shown to attenuate the development of the modeled disease (13, 14). Therefore, given that pulmonary fibrosis is associated with an increased risk for lung cancer (15), we herein aimed to further investigate the potential involvement of the ATX/LPA axis in lung cancer pathogenesis. *ENPP2* was *in silico* discovered to be genetically altered in some patients with lung cancer, whereas increased ATX staining and activity were detected in patients and animal models, accompanied by a downregulation of *PLPP3* expression. Most importantly, genetic deletion of *Enpp2* or *Lpar1* in mice resulted in disease attenuation, thus confirming a procarcinogenic role of ATX/LPA in the lung.

Materials and Methods

Human patients

Demographics and clinicopathological characteristics of patients and controls are presented at Supplementary Tables S1 and S2. Clinical investigations were conducted according to the principles of the Declaration of Helsinki, after approval by an Institutional Review Board. All patients and controls consented in writing for anonymous research usage of their biological samples.

Mice

All mice were bred under specific pathogen-free conditions in their respective genetic backgrounds for over 10 generations at the animal facilities of the Alexander Fleming Biomedical Sciences Research Center. Mice were housed at 20–22°C, 55% ± 5% humidity, and a 12-h light-dark cycle; water and food were given *ad libitum*. All reported experimentation in mice for this project, in line with the ARRIVE guidelines, was approved by the Institutional Animal Ethical Committee of BSRC Alexander Fleming and the Veterinary service and Fishery Department of the local governmental prefecture. All randomly-assigned experimental controls were littermate sex- and age-matched mice.

The generation and genotyping protocols for *Enpp2*$^{n/n}$ (9), *Lpar1*$^{-/-}$ (16), *Lpar2*$^{-/-}$ (17), *K-ras*$^{G12D/+}$ (18), Tg*CC10-Cre* and Tg*LysM-Cre* (14) have been described previously. All mice, except for *Lpar1*$^{-/-}$, were bred in a C57BL/6J genetic background. The oncogenic allele of *K-ras* (G12D; ref. 18) was activated upon the intratracheal delivery of 2.5×10^7 pfu/mouse of an adenovirus expressing Cre recombinase, as previously reported (19) and as described in detail in an Online Data Supplement. Chemically induced lung cancer was provoked upon weekly intraperitoneal (i.p.) injections of 1 g/Kg urethane (URE; ethyl carbamate) for ten consecutive weeks, as previously reported (20) and as described in an Online Data Supplement.

Histology, immunohistochemistry, ATX activity assay (TOOS), HPLC-ESI/MS/MS lipid analysis, RNA Extraction and Real-time RT-PCR were performed essentially as previously reported (12, 14, 20, 21) and as detailed in an Online Data Supplement.

Microarray hybridization and expression data analysis are described in an Online Data Supplement. The MIAME-compliant dataset is publicly available (#E-MTAB-6706) at ArrayExpress.

Statistical analysis

Unless otherwise indicated, statistical significance was estimated through pair-wise comparisons with control values using an unpaired, two-sided Student *t* test or with a Mann-Whitney Rank Sum Test in cases of not normal distribution.

Results

ENPP2 is genetically altered in 8% of patients with lung cancer

To explore a possible role of the ATX/LPA axis in lung cancer, we first examined the genomic status of *ENPP2*, as well as of *LPAR*s and *PLPP*s, in patients with lung cancer. Genomic Identification of Significant Targets in Cancer (GISTIC) analysis was performed online in cBioPortal (22) on publicly available whole-exome sequencing data from the recent landmark genomic study of lung cancer (23), as deposited to The Cancer Genome Atlas (TCGA). *ENPP2* was found genetically altered in 8% of patients with lung cancer ($n = 1{,}144$; Supplementary Fig. S1A); almost 50% of the identified alterations were gene amplifications that were accompanied by *MYC*, as well as other genes in the 8q24 genomic locus, amplification in the same patients (Supplementary Fig. S1B). Alterations in other genes of the ATX/LPA axis were much fewer (Supplementary Fig. S1A).

To assess steady-state mRNA expression of *ENPP2*, as well as *LPAR*s and *PLPP*s, in human lung cancer patients' lung tissue, we performed data mining in 41 lung cancer patient microarray datasets publicly available at NCBI/GEO (Supplementary Table S1) with the embedded tool GEO2R. In sharp contrast with a similar *in silico* query in HCC (12), *ENPP2* mRNA expression was found to be statistically significantly downregulated in lung cancer samples, as compared with controls, in most of the patient cohorts' datasets (Supplementary Table S1 and Supplementary Fig. S2A). *PLPP3* expression in patients with lung cancer was consistently found downregulated, as previously shown with the same methodology in patients with HCC (12). Identical results were obtained from qRT-PCR analysis of 14 patients with NSCLC paired lung samples, where *ENPP2* and *PLPP3* mRNA expression was found lower in cancer biopsies as compared with adjacent healthy lung tissue isolated from the same patients (Supplementary Fig. S2B), thus suggesting deregulated LPA metabolism in patients with lung cancer.

Increased ATX protein levels in the lungs of patients with lung cancer and animal models

To examine pulmonary ATX protein levels, we performed ATX immunohistochemistry in lung tissue biopsies of 281 patients with lung cancer (Table 1), in comparison with 10 healthy controls, spotted in a tissue microarray (TMA) to ensure identical procedures and facilitate direct comparisons. As previously shown

Published OnlineFirst May 3, 2018; DOI: 10.1158/0008-5472.CAN-17-3797

Table 1. Clinicopathological characteristics of patients with lung cancer with microarrayed tissue samples

Variables	*n* (m/f)	Low ATX *n* (m/f)	High ATX *n* (m/f)	χ^2	*P*
Age				0.506	0.477
<64 years	136 (115/21)	58 (48/10)	78 (67/11)		
≥64 years	145 (131/14)	69 (60/9)	76 (71/5)		
Gender				0.673	0.412
Female	35	19	16		
Male	246	108	138		
Smoking				0.0923	0.761
Yes	226 (208/18)	105 (94/11)	121 (114/7)		
No	23 (9/14)	12 (4/8)	11 (5/6)		
n/a	32 (29/3)	10 (10/0)	22 (19/3)		
Histological stage				1.736	0.629
I	89 (75/14)	37 (32/5)	52 (43/9)		
II	76 (69/7)	38 (33/5)	38 (36/2)		
III	80 (70/10)	37 (29/8)	43 (41/2)		
IV	31 (27/4)	12 (11/1)	19 (16/3)		
n/a	5 (5/0)	3 (3/0)	2 (2/0)		
T status				4.226	0.238
1	39 (37/2)	12 (11/1)	27 (26/1)		
2	157 (133/24)	77 (63/14)	80 (70/10)		
3	33 (29/4)	15 (13/2)	18 (16/2)		
4	45 (41/4)	20 (18/2)	25 (23/2)		
n/a	7 (6/1)	3 (3/0)	4 (3/1)		
Lymph node status				4.054	0.256
0	116 (99/17)	47 (42/5)	69 (57/12)		
1	84 (76/8)	44 (37/7)	40 (39/1)		
2	69 (60/9)	31 (24/7)	38 (36/2)		
3	5 (4/1)	1 (1/0)	4 (3/1)		
n/a	7 (7/0)	4 (4/0)	3 (3/0)		
Metastasis status				0.321	0.571
0	244 (213/31)	112 (94/18)	132 (119/13)		
1	31 (27/4)	12 (11/1)	19 (16/3)		
n/a	6 (6/0)	3 (3/0)	3 (3/0)		
Histological type				11.841	0.106
NSCLC	275 (241/34)	122 (104/18)	153 (137/16)		
ADC	110 (91/19)	39* (30/9)	71* (61/10)	4.011*	0.045*
SCC	139 (126/13)	68* (59/9)	71* (67/4)		
ADSQ.	3 (3/0)	1 (1/0)	2 (2/0)		
Giant CC	12 (10/2)	7 (7/0)	5 (3/2)		
Large CC	4 (4/0)	2 (2/0)	2 (2/0)		
n/a	7 (7/0)	5 (5/0)	2 (2/0)		
SCLC	4 (4/0)	3 (3/0)	1 (1/0)		
NET	2 (1/1)	2 (1/1)	0 (0/0)		
Histological grade				3.431	0.634
Undifferentiated	11 (9/2)	6 (6/0)	5 (3/2)		
High grade	10 (6/4)	3 (2/1)	7 (4/3)		
Middle grade	106 (91/15)	52 (43/9)	54 (48/6)		
Middle-low grade	12 (10/2)	4 (3/1)	8 (7/1)		
Low grade	117 (108/9)	48 (43/5)	69 (65/4)		
Well different.	10 (8/2)	4 (2/2)	6 (6/0)		
n/a	15 (14/1)	10 (9/1)	5 (5/0)		

NOTE: ATX staining was arbitrarily designated as low (0–1) or high (2 or 3).

Abbreviations: ADC, adenocarcinoma; ADSQ, adenosquamous; CC, cell carcinoma; m/f, males/females; n/a, not available; NET, neuroendocrine tumor; NSCLC, non–small cell lung cancer; SCC, squamous cell carcinoma; SCLC, small-cell lung cancer.

(14), ATX immunostaining in the healthy lung tissue was localized mainly to the bronchial epithelium and to a lesser extent in alveolar macrophages (Fig. 1A). Moderate to intense ATX staining was detected in lung cancer as compared to healthy lung tissue (Fig. 1A–C), found localized in cancer cells and negligible in the surrounding stroma (Fig. 1A). However, no statistically significant associations of the intensity of ATX staining with any demographic or clinicopathological characteristics were observed (Table 1). Moreover, increased serum ATX activity levels, as detected with the TOOS assay on natural LPC substrates, were found in a different patient with lung cancer cohort ($n = 68$) in comparison with control samples ($n = 19$; Supplementary Table S2). Therefore, lung cancer in humans is associated with increased levels of ATX protein and activity, corroborating a possible involvement of the ATX/LPA axis in lung cancer pathogenesis.

Remarkably, a similarly paradoxical ATX expression profile was detected as well in two animal models of lung cancer, the genetically engineered model of the conditionally activated *K-ras*^{G12D} oncogene (18) and the URE-induced chemical carcinogenesis model (20). In both these models ATX staining was detected in lung cancer cells (Fig. 2A and B; Supplementary Fig. S3A and S3B), whereas ATX activity levels were found

Published OnlineFirst May 3, 2018; DOI: 10.1158/0008-5472.CAN-17-3797

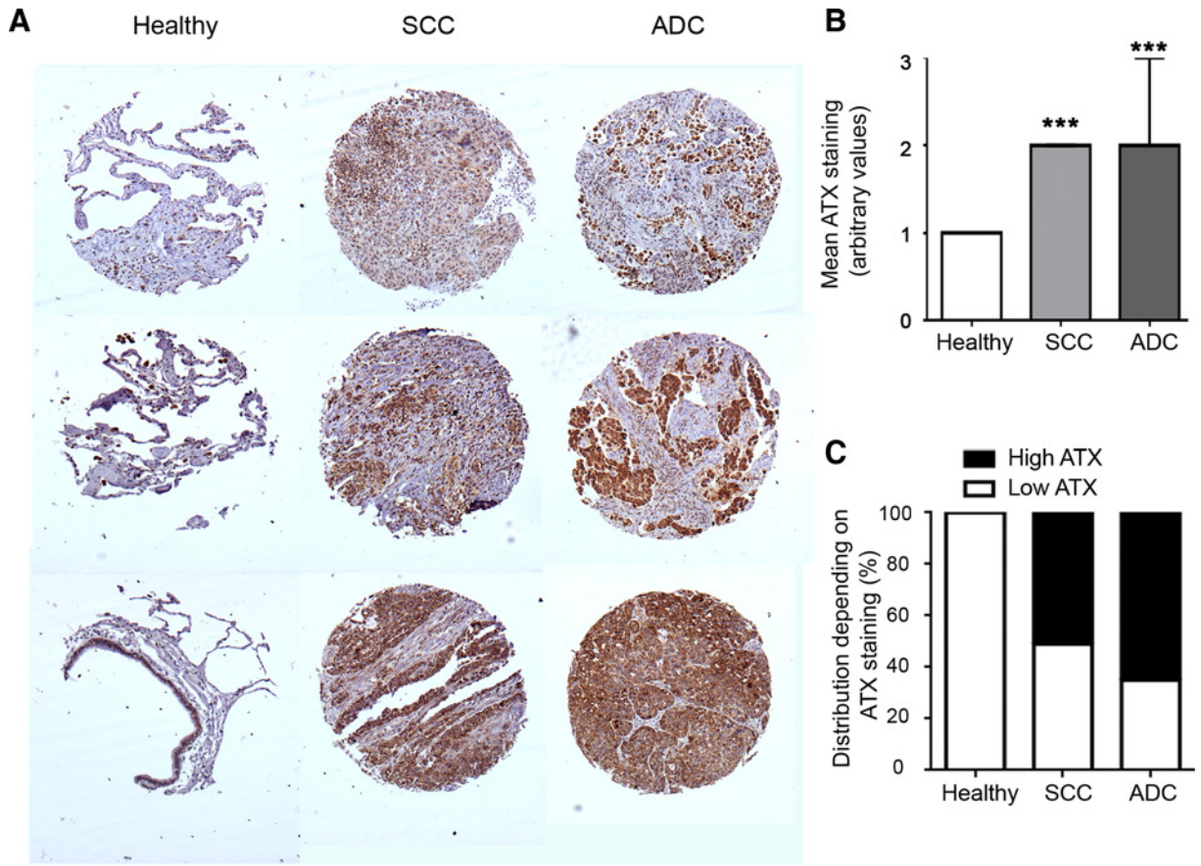

Figure 1.

Increased pulmonary ATX staining in patients with lung cancer. A tissue microarray, composed of mainly NSCLC lung tissue samples as well as control samples, was immunostained for ATX. **A,** Representative images (×100) from healthy ($n = 10$), SCC ($n = 139$) or ADC ($n = 110$) tissue samples stained for ATX. **B,** ATX staining quantification attributing arbitrary intensity values ranging between 0 and 3. Statistical significance was assessed with a Wilcoxon-signed rank test; median values ± interquartile range are shown. ***, $P < 0.001$ over control values. **C,** The percentage of distribution of samples exhibiting low (0–1) or high (2–3) ATX staining. Staining scoring, patient's clinicopathological characteristics and their correlations are shown in Table 1.

increased in the BALFs of the same mice (Fig. 2C and D), correlating with total protein levels (Fig. 2E and F; $r^2 = 0{,}79/0{,}78$, $P = 0.001/0.002$, respectively). In the *K-ras*^{G12D}–driven model, unlike the URE-induced one, higher ATX activity levels were also observed in the plasma (Fig. 2G and H). In sharp contrast, pulmonary *Enpp2*, as well as *Plpp3*, mRNA expression was found downregulated in both animal models (Supplementary Fig. S4A–S4D), as shown for human patients. No major changes in the expression profile of LPARs was noted (Supplementary Fig. S4E and S4F).

Conditional genetic deletion of *Enpp2* from bronchial epithelial cells and macrophages diminishes URE-induced early neoplastic lesions

To examine whether the observed increased pulmonary ATX levels in lung cancer play a functional role in lung carcinogenesis, *Enpp2* was conditionally deleted from bronchial epithelial cells and macrophages, the main pulmonary cells expressing ATX (14). To this end, *Enpp2*$^{n/n}$ mice (9) were mated with transgenic mouse strains expressing the *Cre* recombinase under the control of the *CC10* (*Scgb1a1*) or the *LysM* promoters (14). As previously shown, CC10/LysM-directed genetic deletion of ATX, as verified with recombination assays, did not have any appreciable effects on lung development and architecture under healthy conditions (14). URE (1 g/Kg) was then injected intraperitoneally (IP) for 10 consecutive weeks to C57BL6/J *CC10Enpp2*$^{-/-}$or *LysMEnpp2*$^{-/-}$mice, as well as to control littermates (*Enpp2*$^{n/n}$), and disease severity was examined 15 weeks after the last injection.

As expected (20), all control mice that received URE developed neoplastic lesions (100% incidence), ranging from atypical adenomatous hyperplasias (AAH) to adenomas (AD; Fig. 3A). Inflammation was not a prominent histopathologic feature, although many macrophages (giant cells) were noted near AAH lesions (Fig. 3A). Genetic deletion of *Enpp2* in both *CC10Enpp2*$^{-/-}$or *LysMEnpp2*$^{-/-}$mice resulted in a statistically significant decrease in the number of URE-induced AAH (Fig. 3B and C), indicating a role for pulmonary ATX expression at the initial phases of URE-induced carcinogenesis. However, no statistically significant decreases in the number of AD were noted (Fig. 3D and E); moreover, the genetic deletions diminished but did not attenuate ATX BALF levels (Fig. 3F and G), suggesting extra-pulmonary sources of ATX.

Published OnlineFirst May 3, 2018; DOI: 10.1158/0008-5472.CAN-17-3797

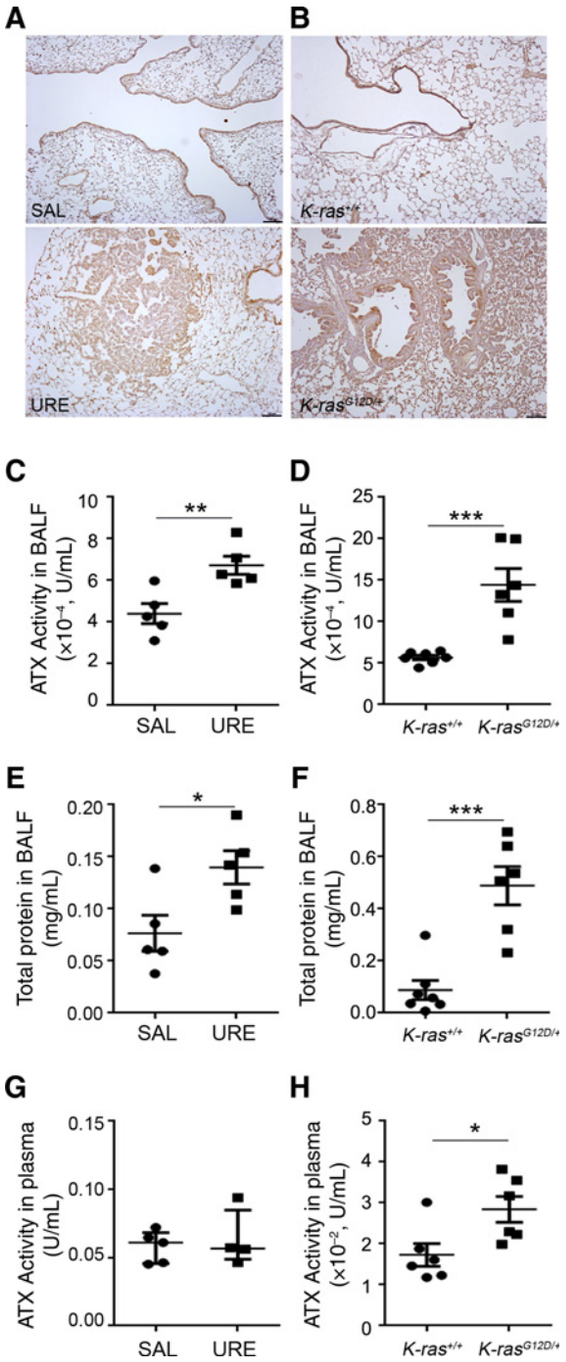

Figure 2.

Increased pulmonary ATX levels in animal models of lung cancer (**A, C, E,** and **G,** URE-induced model; **B, D, F,** and **H,** *K-ras*^{G12D}-driven model). **A** and **B,** Representative ATX immunostaining images from control (**A**, SAL; **B**, *K-ras*$^{+/+}$) or cancer (**A**, URE; **B**, *K-ras*$^{G12D/+}$) lung tissue samples. Additional images are shown in Supplementary Fig. S3. **C** and **D,** ATX activity levels in BALFs, as measured with the TOOS assay. **E** and **F,** Total protein levels in BALFs, as determined with the Bradford assay. **G** and **H,** ATX activity levels in plasmas, as measured with the TOOS assay. Statistical significance was assessed with the unpaired *t* test (**C–F**, and **H**; mean values ± SEM are shown) or Mann–Whitney rank sum test (**G**; median values ± interquartile range are shown); $n = 5$–7 for each experimental group and panel. *, $P < 0.05$; **, $P < 0.01$; ***, $P < 0.001$.

Ubiquitous genetic deletion of *Lpar1*, but not *Lpar2*, attenuates URE-induced carcinogenesis

Genetic deletion of *Lpar1* has been shown to attenuate the development of bleomycin-induced pulmonary fibrosis (13), as was also shown for ATX (14), whereas pulmonary fibrosis is associated with an increased risk for lung cancer (15). Therefore, we next examined a possible contribution of LPAR1 in lung cancer development, through the administration of URE to *Lpar1*$^{-/-}$ mice and their WT littermates. It should be noted that since C57BL/6J *Lpar1*$^{-/-}$ mice are embryonically lethal (data not shown and ref. 16), *Lpar1*$^{-/-}$ mice were bred and maintained on a mixed C57BL/6J/129 genetic background, which is known to be more susceptible to URE-induced carcinogenesis (24). In accordance, WT C57BL/6J/129 mice developed an increased number of ADs, as compared to WT C57BL/6J mice, upon URE administration (Fig. 4A–C). Deletion of *Lpar1* resulted in a reduction of the numbers of URE-induced ADs (Fig. 4C), confirming the participation of the ATX/LPA axis in lung cancer development. On the contrary, no such effect was observed in C57BL/6J *Lpar2*$^{-/-}$ mice (Fig. 4D–F), perhaps in line with a suggested anti-inflammatory role for LPAR2 in allergic airway inflammation (25).

Enpp2 stochastic deletion in pulmonary cells diminishes BALF LPA levels and *K-ras*^{G12D}–driven carcinogenesis

To confirm the procarcinogenic role of the ATX/LPA axis in another animal model of lung cancer, we next used the genetically engineered model of *K-ras*$^{G12D/+}$(18). A replication-deficient adenovirus expressing the *cre* recombinase (Ad-Cre) was administered intratracheally to *K-ras*$^{LSL\text{-}G12D/+}$*Enpp2*$^{n/n}$mice, as well as to control *K-ras*$^{LSL\text{-}G12D/+}$littermates, thus removing the synthetic stop element (LSL; lox-stop-lox) and allowing the expression of the oncogene and the overtime development of lung cancer, ranging from AAH to AD and ADC (18). At the same time, the adenoviral-delivered *cre* also deleted *Enpp2* in the infected cells. Mice were then sacrificed 8 or 16 weeks post Ad-Cre administration and examined for neoplastic lesions (Fig. 5A and B). The stochastic genetic deletion of *Enpp2* from pulmonary cells resulted in a significant reduction of AAHs at both time points (Fig. 5C and D), confirming the results from the URE model. A statistically non-significant reduction of ADs was observed at 8w post Ad-Cre administration, but not at 16w (Fig. 5E and F).

Noteworthy, the effect of the *Enpp2* genetic deletion on ATX BALF levels in *K-ras*$^{G12D/+}$*Enpp2*$^{-/-}$mice was prominent at 8w post Ad-Cre administration but negligible at 16w (Fig. G and H), suggesting that pulmonary cells have a significant contribution to ATX BALF levels at the initial phases of lung cancer development, likely complemented by extra-pulmonary sources at the late stages. In accordance, LPC levels, as measured with LC/MS/MS, were almost doubled in BALFs at 8w post lung cancer induction (Fig. 5I), and diminished in the corresponding plasmas (Fig. 5J); noteworthy, LPC has been shown to be a potent inducer of ATX expression in hepatocytes (12). BALF LPA levels were found increased at 16w in BALFs but not plasmas (Fig. 5K and L), indicating a role for LPA in *K-ras*^{G12D}–driven lung cancer pathogenesis and stressing the importance of the downregulated PLPP3 levels, observed at this time point (Supplementary Fig. S4D), in LPA metabolism and lung cancer development. LPA levels were found diminished upon *Enpp2* genetic deletion (Fig. 5K), reconfirming the key role of ATX in extracellular LPA production.

Published OnlineFirst May 3, 2018; DOI: 10.1158/0008-5472.CAN-17-3797

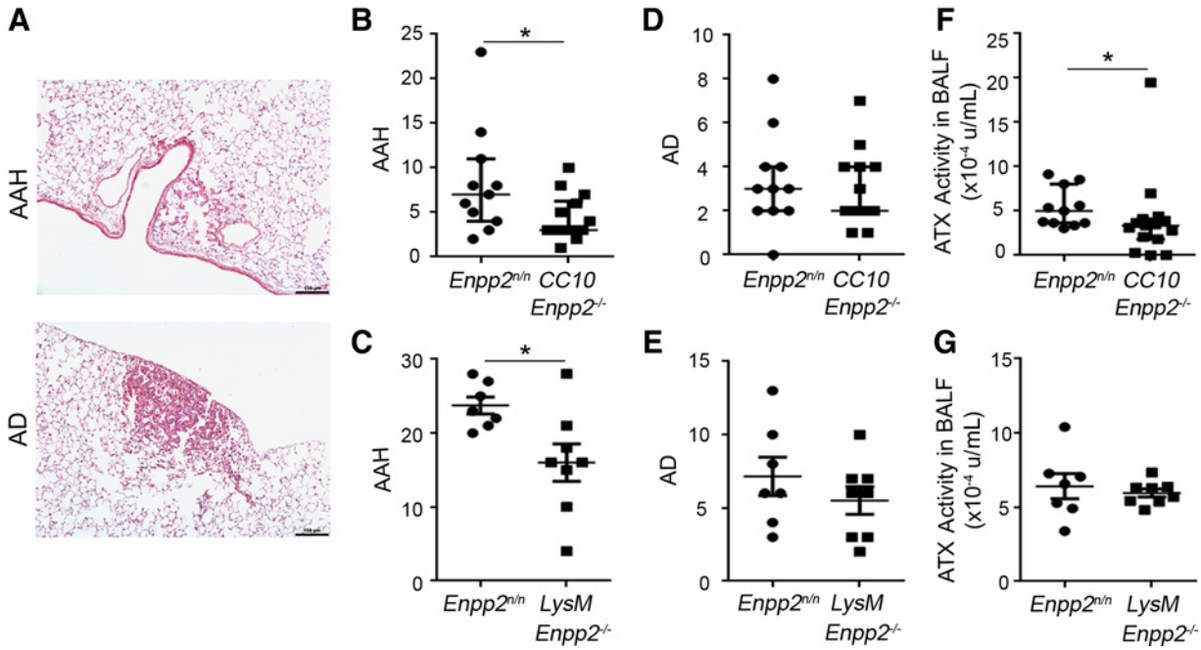

Figure 3.

Conditional genetic deletion of *Enpp2* from bronchial epithelial cells or macrophages diminishes urethane-induced early neoplastic lesions in the lung. **A,** Representative images from hematoxylin and eosin–stained lung tissue sections, indicating atypical AAHs or ADs; their numbers were counted in each mouse in four transverse sections spanning each lung. URE-induced AAH (**B** and **C**) or AD (**D** and **E**) in the indicated groups of mice/genotypes. **F** and **G,** ATX activity levels in BALFs, as measured with the TOOS assay. Statistical significance was assessed with the Mann–Whitney rank sum test (**B, D,** and **F**; $n = 11$–15; median values ± interquartile range are shown) or unpaired t test (**C, E,** and **G**; $n = 7$–8; mean values ± SEM are shown). *, $P < 0.05$.

Mechanistic insights on the role of ATX/LPA in *K-ras*^{G12D}–driven lung cancer pathogenesis

Consistent with the reported LPA effects in various cell types *in vitro* (4, 26), genetic deletion of *Enpp2* and the attenuation of LPA levels resulted in a decrease in the proliferation of cancer cells, as assessed with PCNA staining, as well as a similar decrease in VEGFR2 staining, a marker of angiogenesis (Fig. 6A–D, respectively). However, no major changes were observed in p53 and PTEN staining (data not shown), that their levels have been suggested to be modulated from LPA in lung cancer cell lines *in vitro*.

To obtain additional mechanistic insights into the mode of action of ATX/LPA in *K-ras*^{G12D}–driven lung cancer pathogenesis, we performed mRNA expression profiling in whole lungs of *K-ras*$^{G12D/+}$*Enpp2*$^{+/+}$and *K-ras*$^{G12D/+}$*Enpp2*$^{-/-}$mice 16w post induction. Limited by the heterogeneity of the cancerous lungs and the relatively small spread of cancer cells, 303 *bona fide* deregulated genes were identified (Supplementary Table S3; Fold change > 1.5; $P < 0.05$); only 60 out of them were found upregulated. Interestingly, gene set enrichment analysis indicated that, in the relative absence of ATX and upon lower LPA levels, the 243 downregulated genes were enriched in metabolic genes, including lipid metabolism (Supplementary Table S4). Therefore, these results suggest that the procarcinogenic effects of the ATX/LPA axis in lung cancer pathogenesis include metabolic rewiring, as was recently suggested for HCC (12). However, further studies are required to validate and dissect this intriguing hypothesis, that has multiple implications in LPA physiology and cancer biology.

Discussion

The *ENPP2* gene resides in the human chromosomal region 8q24, one of the most frequent regions of somatic copy number alterations (SCNA; ref. 27) and a region that contains potential susceptibility loci for various cancers, including lung cancer (28). The 8q24 locus has been suggested to regulate the expression of the proto-oncogene *MYC* (29), whereas LPA has been reported to stimulate *Myc* expression and was suggested to cooperate with it in cell transformation (30). Here, *ENPP2* was *in silico* discovered to be genetically altered in 8% of a large cohort of patients with lung cancer (Supplementary Fig. S1), co-amplified, in 50% of the cases, with *MYC* that resides in the same region, one of the most frequently focally amplified genes in lung ADC (23). However, *ENPP2* mRNA expression was found lower in cancerous biopsies than in normal lung tissue, in most patients with lung cancer cohorts' datasets and all samples examined (Supplementary Table S1 and Supplementary Fig. S2). Noteworthy, *ENPP2* was also reported as underexpressed in breast carcinomas despite a detected gene amplification, most likely due to the observed hypermethylation in promoter regions of the gene (8, 31), suggesting that epigenetic modifications could also downregulate ATX mRNA levels at the terminal stages of lung cancer.

Striking immunostaining for ATX, which has been scrutinized elsewhere (12, 14, 21), was detected in both ADCs and SCCs (Fig. 1). However, and given the reported downregulated *ENPP2* mRNA levels in lung cancer, it is unlikely that the observed increased ATX levels are derived from the cancer cells themselves, as previously reported for breast cancer (32). ATX has been shown to engage integrins β1 and β3 at the surface of platelets and cancer

Published OnlineFirst May 3, 2018; DOI: 10.1158/0008-5472.CAN-17-3797

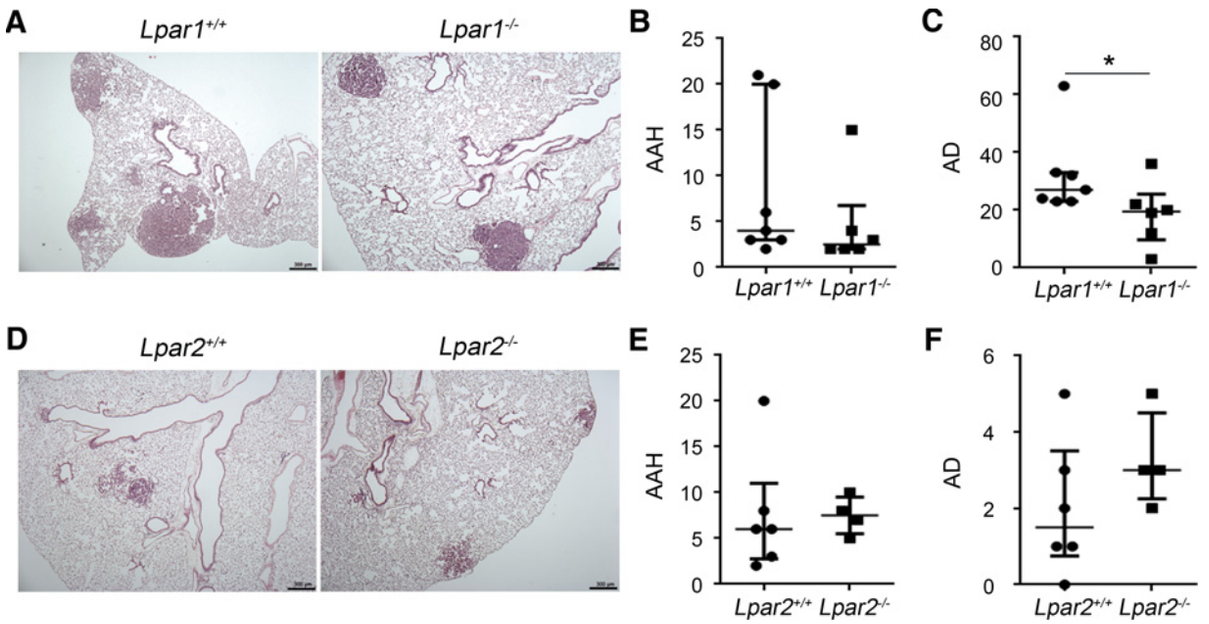

Figure 4.

Genetic deletion of *Lpar1*, but not *Lpar2*, attenuates urethane-induced lung neoplasias. **A** and **D,** Representative images from hematoxylin and eosin–stained lung tissue sections from the indicated mice/genotypes post urethane administration. The numbers of URE-induced atypical AAHs or ADs were counted in each mouse in four transverse sections spanning each lung. URE-induced AAH (**B** and **E**) or AD (**C** and **F**) in the indicated groups of mice/genotypes. Statistical significance was assessed with the Mann–Whitney rank sum test; $n = 4$–7; median values ± IQR are shown; *, $P < 0.05$.

cells (33–35), both of which correlate with short survival in patients with early NSCLC (36) and participate in heterodimers associated with disease progression in various cancers (37). Therefore, it cannot be excluded that locally secreted or extravasated ATX can bind to the surface of lung cancer cells via integrins, thus avoiding clearance while exerting locally produced LPA effects and establishing a permissive microenvironment for cancer growth. In addition, *PLPP3* expression was discovered to be lower in all lung cancer datasets and samples examined (Supplementary Table S1 and Supplementary Fig. S2), suggesting an additional mechanism to maintain high levels of LPA on the surface of tumor cells, because PLPP3 is a transmembrane protein shown to degrade extracellular LPA (5).

Mouse models for lung cancer are valuable tools for deciphering tumor biology, as well as for the development and validation of new tumor intervention strategies. In this study, we employed the two most widely used, the carcinogen (URE)–induced and the genetically engineered *K-Ras*^{G12D}-driven, that represent the two major types of human lung cancer from a genomic perspective, one principally with somatic mutations and the other with SCNAs respectively (27, 38). Identical results regarding *Enpp2* expression have been obtained in both models, remarkably phenocopying the human data: increased ATX activity was measured in BALFs and ATX staining was detected in cancer cells (Fig. 2); however, *Enpp2*, as well as *Plpp3*, mRNA levels were found downregulated in whole lung samples (Supplementary Fig. S4). Importantly, the mouse studies revealed that ATX levels correlated with total protein in BALFs, indicative of endothelial permeability and pulmonary edema, suggesting that a large part of pulmonary ATX derives from the circulation during carcinogenesis. Moreover, ATX has been reported to be released from human platelets upon tumor cell–induced aggregation (35), suggesting an additional possible source of ATX. Noteworthy, 40% of plasma ATX is thought to derive from the adipose tissue (39), known to secrete various hormones and cytokines (adipokines) that exhibit significant systemic effects on various pathophysiological processes, including lipid metabolism, inflammation, and cancer (40).

Genetic deletion of *Enpp2* from its major pulmonary source—the bronchial epithelium (CC10^{+}), as well as from monocytic (LysM^{+}) cells, resulted in a marked reduction of AAHs (Fig. 3), the first neoplastic lesions that develop upon carcinogen-induced carcinogenesis. Comparable results were obtained upon the stochastic genetic deletion of *Enpp2* in pulmonary (most likely epithelial) cells upon *K-ras*^{G12D}-driven lung carcinogenesis (Fig. 5), suggesting that local pulmonary ATX expression plays a role in tumor initiation. ATX deletion was accompanied by lower LPA BALF levels (Fig. 5), reaffirming that ATX exerts its effects through the local production of LPA. It has been proposed that LPA can downregulate ATX expression levels in some cells and conditions (41), providing an additional explanation for the low *Enpp2* mRNA levels at the terminal stages of both human (Supplementary Table S1 and Supplementary Fig. S2) and mouse (Supplementary Fig. S4) lung cancer. LPA levels remained high most likely due to the enzymatic action of extravasated ATX and/or due to a marked reduction in *Plpp3* expression upon carcinogenesis (Supplementary Fig. S4).

The genetic deletion of ATX from pulmonary cells in both models did not result in a significant reduction in AD development, most likely due to the recruitment of ATX from the circulation that complements or even outweighs local pulmonary expression. However, the participation of the ATX/LPA axis in lung cancer development was ultimately proven in *Lpar1* knock

Published OnlineFirst May 3, 2018; DOI: 10.1158/0008-5472.CAN-17-3797

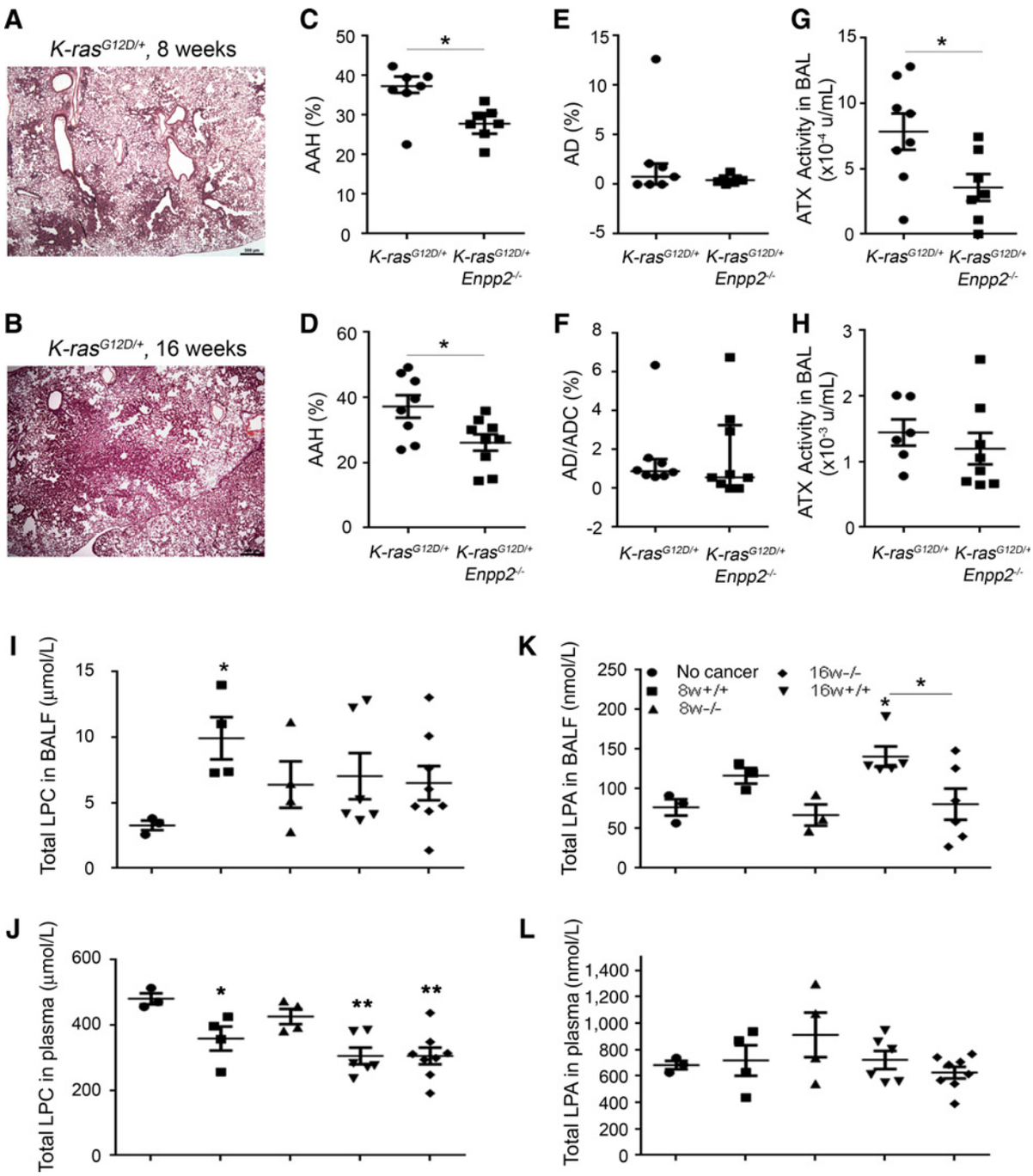

Figure 5.

Stochastic genetic deletion of *Enpp2* from pulmonary cells diminishes *K-ras*^{G12D}–driven neoplasias. *K-ras*^{G12D}–driven lung carcinogenesis was assessed in the presence or absence of *Enpp2*, 8w (**A**, **C**, **E**, and **G**) or 16 w (**B**, **D**, **F**, and **H**) post Ad-Cre administration and oncogene activation. **A** and **B,** Representative images from hematoxylin and eosin–stained lung tissue sections 8w and 16w post oncogene activation. The numbers of *K-ras*^{G12D}–driven AAHs, ADs, or ADCs were counted in each mouse in four transverse sections spanning each lung. *K-ras*^{G12D}–driven AAH (**C** and **D**) or AD/ADC (**E** and **F**) in the indicated groups of mice/genotypes. **G** and **H,** ATX activity levels in BALFs, as determined with the TOOS assay. Total levels of LPC or LPA in BALF (**I** and **K**, respectively) and plasma (**J** and **L**, respectively) at both time points. Statistical significance was assessed with Mann–Whitney rank sum test (**C, E,** and **F**; median values ± interquartile range are shown), unpaired *t* test (**D, G,** and **H**; mean values ± SEM are shown) or one-way ANOVA and Fischer's LSD as a *post-hoc* test (**I–L**; mean values ± SEM are shown). **A–H,** $n = 6–9$; **I–L,** $n = 3–8$; *, $P < 0.05$.

Published OnlineFirst May 3, 2018; DOI: 10.1158/0008-5472.CAN-17-3797

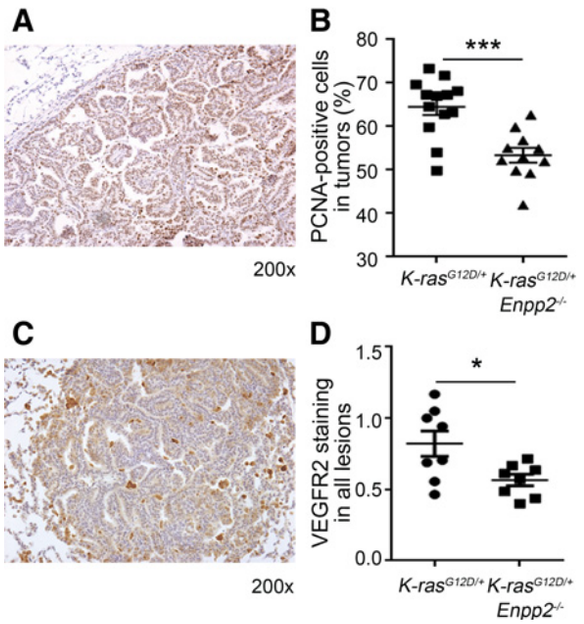

Figure 6.

Decreased proliferation and angiogenesis upon stochastic genetic deletion of *Enpp2* from pulmonary cells. **A** and **B,** Nuclear staining for proliferation marker PCNA is decreased in the lung tumors of *K-ras*$^{G12D/+}$*Enpp2*$^{-/-}$ mice compared with the staining in the tumors of *K-ras*$^{G12D/+}$ mice. A representative image of PCNA tumor staining is shown in **A**. Quantification of tumoral staining is presented as a percentage of stained cells over total cell number and is depicted in **B**; total optical fields assessed per group, $n = 11$–13. **C** and **D,** Staining for angiogenesis marker VEGFR2 in both early and late neoplastic lesions is lower in *K-ras*$^{G12D/+}$*Enpp2*$^{-/-}$ than *K-ras*$^{G12D/+}$ mice. A representative image of VEGFR2 tumoral staining is shown in **C**. Quantification of staining is presented in **D**, showing mean values of optical fields from each mouse and their total mean values ± SEM; $n = 8$. Statistical significance was assessed with unpaired *t* test; *, $P < 0.05$; ***, $P < 0.001$.

out mice, where a significant decrease of ADs upon URE-induced carcinogenesis was observed (Fig. 4). LPAR1 expression and signaling has been also shown as a pathogenic determinant of pulmonary fibrosis (13); therefore, these results further extend the similarities between lung fibrosis and cancer (15). LPAR2, which is hardly expressed in pulmonary cells (Supplementary Fig. S4; ref. 7), was shown to have minor effects in URE-induced lung cancer (Fig. 4). LPAR6 is highly expressed in the liver and HCC (12, 42) and has been shown to support liver tumorigenesis (42). LPAR6 is also the highest expressing LPAR in the lung (Supplementary Fig. S4), but its role in pulmonary pathophysiology has not been explored yet.

LPAR1 couples to at least three distinct G proteins (G_q, G_i and $G_{12/13}$), which in turn feed into multiple effector pathways, including activation of the mitogen-activated protein kinases (MAPK) and phosphatidylinositol 3-kinase (PI3K) cascades, leading to cytoskeletal rearrangements and to increased proliferation (Fig. 6) and motility (4, 6, 7, 26). Noteworthy, these LPA-stimulated signaling pathways are shared with many of the established players and therapeutic targets in lung carcinogenesis, such as K-RAS and EGFR. Therefore, costimulation by LPAR1 and its associated G-proteins could lower their activation thresholds, thus promoting disease initiation and progression. In addition to these direct effects to cancer cells, LPA has been also suggested to regulate angiogenesis (Fig. 6; ref. 43), as well as pulmonary vascular leak (13), facilitating the influx of inflammatory and growth factors. An involvement of the ATX/LPA axis in cancer immunoregulation is also likely, since ATX has been reported to adhere to lymphocytes facilitating their homing (44), whereas increased ATX staining has been reported at lymphoid aggregates in patients tissue, including NSCLC (21, 45). Moreover, all immune cells were shown to possess some LPARs, and LPA has been recently proposed to convert monocytes into macrophages (46).

Beyond these established or suggested ATX/LPA effects in various hallmarks of cancer, a novel metabolic function of the axis in carcinogenesis is emerging. ATX/LPA were recently shown, both *in vitro* and *in vivo*, to play a role in liver lipid metabolism during HCC development, regulating triglyceride (TGA) levels (12). Expression profiling of modeled HCC in the absence of hepatocyte ATX expression, indicated genes that are involved in lipid metabolism (12). Intriguingly, similar deregulated metabolic pathways were also discovered in lung cancer (Supplementary Table S4), and several related liver specific genes were found activated by ATX/LPA in the lung (Supplementary Table S3), suggesting that LPA-induced metabolic rewiring is not confined to the liver. However, further studies are needed to establish a direct causative relationship and to dissect a possible involvement of these complex and redundant pathways. Finally, many genes involved in drug metabolism and/or resistance were discovered to be affected by ATX/LPA during lung (Supplementary Tables S3 and S4) and liver (12) carcinogenesis. Accordingly, ATX has been suggested to protect cancer cells from taxol-induced apoptosis (47) and to mediate the acquired resistance against sunitinib, cisplatin and adriamycin (48, 49). Moreover, LPA signaling was shown to induce the Nrf2-mediated expression of multi-drug resistance transporters and antioxidant genes (50), suggesting that therapeutic targeting of the ATX/LPA axis could be useful as an adjuvant therapy.

In summary, strong indications on a possible involvement of the ATX/PLPP3-LPA/LPAR1 axis in lung carcinogenesis, in both human patients and mouse animal models were provided. Furthermore, genetic deletion of *Enpp2* and *Lpar1* was shown to attenuate cancer development in animal models, thus establishing a procarcinogenic role of the axis in lung cancer pathogenesis, expanding the mechanistic links of pulmonary fibrosis and cancer, while further revealing possible LPA effects in tumor metabolism, an emerging hallmark.

Disclosure of Potential Conflicts of Interest

No potential conflicts of interest were disclosed.

Authors' Contributions

Conception and design: D. Bouros, K. Syrigos, V. Aidinis

Development of methodology: C. Magkrioti, N. Oikonomou, G.T. Stathopoulos, E. Bouros, D. Bouros

Acquisition of data (provided animals, acquired and managed patients, provided facilities, etc.): C. Magkrioti, N. Oikonomou, E. Kaffe, M.-A. Mouratis, I. Barbayianni, V. Harokopos, C. Valavanis, J. Chun, A. Kosma, E. Bouros, D. Bouros, K. Syrigos

Analysis and interpretation of data (e.g., statistical analysis, biostatistics, computational analysis): C. Magkrioti, N. Oikonomou, E. Kaffe, M.-A. Mouratis, V. Harokopos, C. Valavanis, G.T. Stathopoulos, K. Syrigos

Writing, review, and/or revision of the manuscript: C. Magkrioti, M.-A. Mouratis, J. Chun, E. Bouros, D. Bouros, K. Syrigos, V. Aidinis

Administrative, technical, or material support (i.e., reporting or organizing data, constructing databases): C. Magkrioti, N. Xylourgidis, I. Barbayianni, P. Megadoukas
Study supervision: D. Bouros, K. Syrigos, V. Aidinis
Other (performing immunohistochemistry evaluation of human and mouse pathology and immunohistochemical data): C. Valavanis

Acknowledgments

This research has been co-financed in part by the European Union (European Regional Development Fund) and Greek national funds through the National Strategic Reference Framework (NSRF) and the Operational Programs "Competitiveness and Entrepreneurship" (#09SYN-11-679 and 09SYN-12-680 to V. Aidinis; MIS 5002562 to BSRC Fleming), as well as the National co-funding of European programs (#2006ΣΕ01330024—ΣΑΕ 013/3). C. Magkrioti was supported by a scholarship from the State Scholarships Foundation (#4688; IKY/Siemens-excellence).

The costs of publication of this article were defrayed in part by the payment of page charges. This article must therefore be hereby marked *advertisement* in accordance with 18 U.S.C. Section 1734 solely to indicate this fact.

Received December 7, 2017; revised March 27, 2018; accepted April 30, 2018; published first May 3, 2018.

References

1. Herbst RS, Heymach JV, Lippman SM. Lung CANCER. N Engl J Med 2008;359:1367–80.
2. Swanton C, Govindan R. Clinical implications of genomic discoveries in lung cancer. N Engl J Med 2016;374:1864–73.
3. The Cancer Genome Atlas Research N. Comprehensive molecular profiling of lung adenocarcinoma. Nature 2014;511:543–50.
4. Barbayianni E, Kaffe E, Aidinis V, Kokotos G. Autotaxin, a secreted lysophospholipase D, as a promising therapeutic target in chronic inflammation and cancer. Prog Lipid Res 2015;58:76–96.
5. Tang X, Benesch MG, Brindley DN. Lipid phosphate phosphatases and their roles in mammalian physiology and pathology. J Lipid Res 2015;56:2048–60.
6. Aikawa S, Hashimoto T, Kano K, Aoki J. Lysophosphatidic acid as a lipid mediator with multiple biological actions. J Biochem 2015;157:81–9.
7. Choi JW, Herr DR, Noguchi K, Yung YC, Lee CW, Mutoh T, et al. LPA receptors: subtypes and biological actions. Annu Rev Pharmacol Toxicol 2010;50:157–86.
8. Benesch MGK, Yang Z, Tang X, Meng G, Brindley DN. Lysophosphatidate Signaling: The Tumor Microenvironment's New Nemesis. Trends in Cancer 2017;3:748–52.
9. Fotopoulou S, Oikonomou N, Grigorieva E, Nikitopoulou I, Paparountas T, Thanassopoulou A, et al. ATX expression and LPA signalling are vital for the development of the nervous system. Dev Biol 2010;339:451–64.
10. Katsifa A, Kaffe E, Nikolaidou-Katsaridou N, Economides AN, Newbigging S, McKerlie C, et al. The Bulk of Autotaxin Activity Is Dispensable for Adult Mouse Life. PLoS One 2015;10:e0143083.
11. Liu S, Umezu-Goto M, Murph M, Lu Y, Liu W, Zhang F, et al. Expression of autotaxin and lysophosphatidic acid receptors increases mammary tumorigenesis, invasion, and metastases. Cancer Cell 2009;15:539–50.
12. Kaffe E, Katsifa A, Xylourgidis N, Ninou I, Zannikou M, Harokopos V, et al. Hepatocyte Autotaxin expression promotes liver fibrosis and cancer. Hepatology 2017;65:1369–1383.
13. Tager AM, LaCamera P, Shea BS, Campanella GS, Selman M, Zhao Z, et al. The lysophosphatidic acid receptor LPA1 links pulmonary fibrosis to lung injury by mediating fibroblast recruitment and vascular leak. Nat Med 2008;14:45–54.
14. Oikonomou N, Mouratis MA, Tzouvelekis A, Kaffe E, Valavanis C, Vilaras G, et al. Pulmonary autotaxin expression contributes to the pathogenesis of pulmonary fibrosis. Am J Respir Cell Mol Biol 2012;47:566–74.
15. King CS, Nathan SD. Idiopathic pulmonary fibrosis: effects and optimal management of comorbidities. Lancet Respir Med 2017;5:72–84.
16. Contos JJ, Fukushima N, Weiner JA, Kaushal D, Chun J. Requirement for the lpA1 lysophosphatidic acid receptor gene in normal suckling behavior. Proc Natl Acad Sci U S A 2000;97:13384–9.
17. Contos JJ, Ishii I, Fukushima N, Kingsbury MA, Ye X, Kawamura S, et al. Characterization of lpa(2) (Edg4) and lpa(1)/lpa(2) (Edg2/Edg4) lysophosphatidic acid receptor knockout mice: signaling deficits without obvious phenotypic abnormality attributable to lpa(2). Mol Cell Biol 2002;22:6921–9.
18. Johnson L, Mercer K, Greenbaum D, Bronson RT, Crowley D, Tuveson DA, et al. Somatic activation of the K-ras oncogene causes early onset lung cancer in mice. Nature 2001;410:1111–6.
19. DuPage M, Dooley AL, Jacks T. Conditional mouse lung cancer models using adenoviral or lentiviral delivery of Cre recombinase. Nat Protoc 2009;4:1064–72.
20. Stathopoulos GT, Sherrill TP, Cheng DS, Scoggins RM, Han W, Polosukhin VV, et al. Epithelial NF-kappaB activation promotes urethane-induced lung carcinogenesis. Proc Natl Acad Sci U S A 2007;104:18514–9.
21. Nikitopoulou I, Oikonomou N, Karouzakis E, Sevastou I, Nikolaidou-Katsaridou N, Zhao Z, et al. Autotaxin expression from synovial fibroblasts is essential for the pathogenesis of modeled arthritis. J Exp Med 2012;209:925–33.
22. Gao J, Aksoy BA, Dogrusoz U, Dresdner G, Gross B, Sumer SO, et al. Integrative analysis of complex cancer genomics and clinical profiles using the cBioPortal. Sci Signal 2013;6:pl1.
23. Campbell JD, Alexandrov A. Distinct patterns of somatic genome alterations in lung adenocarcinomas and squamous cell carcinomas. Nat Genet 2016;48:607–16.
24. Malkinson AM. Genetic studies on lung tumor susceptibility and histogenesis in mice. Environ Health Perspect 1991;93:149–59.
25. Emo J, Meednu N, Chapman TJ, Rezaee F, Balys M, Randall T, et al. Lpa2 is a negative regulator of both dendritic cell activation and murine models of allergic lung inflammation. J Immunol 2012;188:3784–90.
26. Magkrioti C, Aidinis V. ATX and LPA signalling in lung pathophysiology. World J Respirol 2013;3:77–103.
27. Ciriello G, Miller ML, Aksoy BA, Senbabaoglu Y, Schultz N, Sander C. Emerging landscape of oncogenic signatures across human cancers. Nat Genet 2013;45:1127–33.
28. Brisbin AG, Asmann YW, Song H, Tsai YY, Aakre JA, Yang P, et al. Meta-analysis of 8q24 for seven cancers reveals a locus between NOV and ENPP2 associated with cancer development. BMC Med Genet 2011;12:156.
29. Grisanzio C, Freedman ML. Chromosome 8q24-Associated Cancers and MYC. Genes & cancer 2010;1:555–9.
30. Samadi N, Bekele R, Capatos D, Venkatraman G, Sariahmetoglu M, Brindley DN. Regulation of lysophosphatidate signaling by autotaxin and lipid phosphate phosphatases with respect to tumor progression, angiogenesis, metastasis and chemo-resistance. Biochimie 2011;93:61–70.
31. Parris TZ, Kovacs A, Hajizadeh S, Nemes S, Semaan M, Levin M, et al. Frequent MYC coamplification and DNA hypomethylation of multiple genes on 8q in 8p11-p12-amplified breast carcinomas. Oncogenesis 2014;3:e95.
32. Benesch MG, Tang X, Maeda T, Ohhata A, Zhao YY, Kok BP, et al. Inhibition of autotaxin delays breast tumor growth and lung metastasis in mice. Faseb J 2014;28:2655–66.
33. Fulkerson Z, Wu T, Sunkara M, Kooi CV, Morris AJ, Smyth SS. Binding of autotaxin to integrins localizes lysophosphatidic acid production to platelets and mammalian cells. J Biol Chem 2011;286:34654–63.
34. Hausmann J, Kamtekar S, Christodoulou E, Day JE, Wu T, Fulkerson Z, et al. Structural basis of substrate discrimination and integrin binding by autotaxin. Nat Struct Mol Biol 2011;18:198–204.
35. Leblanc R, Lee SC, David M, Bordet JC, Norman DD, Patil R, et al. Interaction of platelet-derived autotaxin with tumor integrin alphaVbeta3 controls metastasis of breast cancer cells to bone. Blood 2014;124:3141–50.
36. Dingemans AM, van den Boogaart V, Vosse BA, van Suylen RJ, Griffioen AW, Thijssen VL. Integrin expression profiling identifies integrin alpha5 and beta1 as prognostic factors in early stage non-small cell lung cancer. Mol Cancer 2010;9:152.
37. Desgrosellier JS, Cheresh DA. Integrins in cancer: biological implications and therapeutic opportunities. Nat Rev Cancer 2010;10:9–22.

Published OnlineFirst May 3, 2018; DOI: 10.1158/0008-5472.CAN-17-3797

38. Westcott PM, Halliwill KD, To MD, Rashid M, Rust AG, Keane TM, et al. The mutational landscapes of genetic and chemical models of Kras-driven lung cancer. Nature 2014;517:489–92.
39. Dusaulcy R, Rancoule C, Gres S, Wanecq E, Colom A, Guigne C, et al. Adipose-specific disruption of autotaxin enhances nutritional fattening and reduces plasma lysophosphatidic acid. J Lipid Res 2011;52: 1247–55.
40. Federico L, Jeong KJ, Vellano CP, Mills GB. Autotaxin, a lysophospholipase D with pleomorphic effects in oncogenesis and cancer progression. J Lipid Res 2016;57:25–35.
41. Benesch MG, Zhao YY, Curtis JM, McMullen TP, Brindley DN. Regulation of autotaxin expression and secretion by lysophosphatidate and sphingosine 1-phosphate. J Lipid Res 2015;56:1134–44.
42. Mao XY, Lee MJ, Zhu J, Zhu C, Law SM, Snijders AM. Genome-wide screen identifies a novel prognostic signature for breast cancer survival. Oncotarget 2017;8:14003–16.
43. Chen Y, Ramakrishnan DP, Ren B. Regulation of angiogenesis by phospholipid lysophosphatidic Acid. Front Biosci 2013;18:852–61.
44. Kanda H, Newton R, Klein R, Morita Y, Gunn MD, Rosen SD. Autotaxin, an ectoenzyme that produces lysophosphatidic acid, promotes the entry of lymphocytes into secondary lymphoid organs. Nat Immunol 2008;9: 415–23.
45. Yang Y, Mou L, Liu N, Tsao MS. Autotaxin expression in non-small-cell lung cancer. Am J Respir Cell Mol Biol 1999;21:216–22.
46. Ray R, Rai V. Lysophosphatidic acid converts monocytes into macrophages in both mice and humans. Blood 2017;129:1177–1183.
47. Samadi N, Gaetano C, Goping IS, Brindley DN. Autotaxin protects MCF-7 breast cancer and MDA-MB-435 melanoma cells against Taxol-induced apoptosis. Oncogene 2009;28:1028–39.
48. Su SC, Hu X, Kenney PA, Merrill MM, Babaian KN, Zhang XY, et al. Autotaxin-lysophosphatidic acid signaling axis mediates tumorigenesis and development of acquired resistance to sunitinib in renal cell carcinoma. Clin Cancer Res 2013;19:6461–72.
49. Shuyu E, Lai YJ, Tsukahara R, Chen CS, Fujiwara Y, Yue J, et al. Lysophosphatidic acid 2 receptor-mediated supramolecular complex formation regulates its antiapoptotic effect. J Biol Chem 2009;284:14558–71.
50. Venkatraman G, Benesch MG, Tang X, Dewald J, McMullen TP, Brindley DN. Lysophosphatidate signaling stabilizes Nrf2 and increases the expression of genes involved in drug resistance and oxidative stress responses: implications for cancer treatment. Faseb J 2014;29:772–85.

Published OnlineFirst May 3, 2018; DOI: 10.1158/0008-5472.CAN-17-3797

Cancer Research
The Journal of Cancer Research (1916–1930) | The American Journal of Cancer (1931–1940)

AACR American Association for Cancer Research

The Autotaxin––Lysophosphatidic Acid Axis Promotes Lung Carcinogenesis

Christiana Magkrioti, Nikos Oikonomou, Eleanna Kaffe, et al.

Cancer Res 2018;78:3634-3644. Published OnlineFirst May 3, 2018.